Fibroblast Growth Factor 2 and Estrogen Control the Balance of Histone 3 Modifications Targeting MAGE-A3 in Pituitary Neoplasia

Xuegong Zhu,[1,3] Sylvia L. Asa,[2,3] and Shereen Ezzat[1,3]

Abstract

Purpose: Four members of the fibroblast growth factor receptor (FGFR) family transduce signals of a diverse group of FGF ligands. The FGFR2-IIIb isoform is abundantly present in the normal pituitary gland with contrasting down-regulation in neoplastic pituitary cells. cDNA profiling identified the cancer-testis antigen melanoma-associated antigen A3 (MAGE-A3) as a putative target negatively regulated by FGFR2.

Experimental Design: Comparisons were made between normal and neoplastic human and mouse pituitary cells. Gene expression was examined by reverse transcription-PCR, DNA methylation was determined by methylation-specific PCR and combined bisulfite restriction analysis, and histone modification marks were identified by chromatin immunoprecipitation.

Results: Normal human pituitary tissue that expresses FGFR2-IIIb does not express MAGE-A3; in contrast, pituitary tumors that are FGFR2 negative show abundant MAGE-A3 mRNA expression. MAGE-A3 expression correlates with the presence and extent of DNA promoter methylation; more frequent and higher-degree methylation is present in the normal gland compared with pituitary tumors. Conversely, pituitary tumors are hypomethylated, particularly in females where MAGE-A3 expression is nearly thrice higher than in males. Estradiol treatment induces MAGE-A3 through enhanced histone 3 acetylation and diminished methylation. The effects of estradiol are directly opposed by FGF7/FGFR2-IIIb. Down-regulation of MAGE-A3 results in p53 transcriptional induction, also through reciprocal histone acetylation and methylation modifications.

Conclusions: These findings highlight MAGE-A3 as a target of FGFR2-IIIb and estrogen action and provide evidence for a common histone-modifying network in the control of the balance between opposing signals.

Pituitary tumors compose nearly 10% of surgically excised intracranial neoplasms. They cause morbidity through invasive growth into surrounding brain and bony structures. Pituitary tumorigenesis infrequently involves intragenic mutations of oncogenes or tumor suppressor genes (1, 2). Mounting evidence suggests that signals implicated in pituitary organogenesis may be relevant to the tumorigenic processes in this gland with major contributions from members of the bone morphogenic protein, Wnt, and fibroblast growth factor (FGF) families (3, 4).

There are currently 23 recognized members of the FGF ligand family and their receptors are encoded by four independent genes each giving rise to multiple isoforms (5). The FGF receptor 2 (*FGFR2*) gene is alternatively spliced to generate FGFR2-IIIb (also referred to as KGFR), an isoform containing the second half of the third immunoglobulin-like domain encoded by exon 7, which binds FGF1, FGF3, FGF7, and FGF10 with high affinity (6, 7). In contrast, the FGFR2-IIIc isoform (also referred to as Bek), in which the second half of the third immunoglobulin-like domain is encoded by exon 8, does not bind FGF7 or FGF10 (8, 9). FGFR2-IIIb expression is tightly restricted to epithelial cells, whereas FGFR2-IIIc is more frequently found in mesenchymal cells (10).

FGF signaling is critical in pituitary development. Deletion of the FGFR2-IIIb isoform leads to failure of pituitary development (11). Midgestational expression of a soluble dominant-negative FGFR results in severe pituitary dysgenesis (12). Similarly, multiple lines of evidence have supported the involvement of members of the FGF/FGFR family in pituitary tumorigenesis. Selected FGF ligands are overexpressed in pituitary tumors (13). Moreover, the human endogenous FGF antisense gene (GFG) is expressed in the normal pituitary where it restricts cell proliferation, and its expression is reduced in pituitary tumors (14).

We have previously shown altered expression of two members of the FGFR family in pituitary tumors (15). We noted that FGFR4 is NH_2-terminally truncated to yield a pituitary tumor-derived FGFR4 (ptd-FGFR4; refs. 15, 16) as a result of alternative transcription initiation from a cryptic intronic promoter (17, 18). This oncogene displaces N-cadherin from the cell membrane to interfere with normal cell adhesion (19). We also observed that FGFR2-IIIb is expressed by the normal pituitary

Authors' Affiliations: [1]Departments of Medicine and [2]Laboratory Medicine and Pathobiology, University of Toronto and [3]The Ontario Cancer Institute, University Health Network, Toronto, Ontario, Canada

Received 8/13/07; revised 12/11/07; accepted 12/20/07.

Grant support: Canadian Institutes of Health Research grant MT-14404 and the Toronto Medical Laboratories.

The costs of publication of this article were defrayed in part by the payment of page charges. This article must therefore be hereby marked *advertisement* in accordance with 18 U.S.C. Section 1734 solely to indicate this fact.

Requests for reprints: Shereen Ezzat, Ontario Cancer Institute, 610 University Avenue, 8-327, Toronto, Ontario, Canada M5G 2M9. Phone: 416-946-4501; Fax: 416-586-8834; E-mail: shereen.ezzat@utoronto.ca.

doi:10.1158/1078-0432.CCR-07-2003

but significantly down-regulated in pituitary tumors (15). Forced expression of FGFR2-IIIb arrests pituitary tumor cell cycle progression (20).

Given the recognized role for FGFR2 in the development of the anterior pituitary gland (1) and the common theme of epigenetic silencing in human pituitary tumorigenesis (21), we examined putative target genes of FGFR2-IIIb using cDNA microarray profiling. Although the expression of the majority of spotted genes was not significantly altered, we found that members of the cancer-testis antigen melanoma-associated antigen A (MAGE-A) were down-regulated by nearly 60-fold (22). These findings prompted us to examine whether MAGE-A3/6 is expressed in human pituitary tumors where FGFR2 is down-regulated and whether this relationship is governed through interdependency on histone modifications.

Materials and Methods

Human pituitary tumor specimens. Normal human pituitary specimens with no morphologic abnormalities and primary human pituitary adenomas were obtained at the time of surgery following informed consent and Institutional Review. The pituitary adenomas were examined and classified according to the accepted Armed Forces Institute of Pathology and WHO criteria (23, 24). Details of these samples are summarized in Supplementary Table S1 and as previously reported (20).

Cell culture and treatment. Mouse pituitary AtT20 corticotroph cells were grown in Ham's F-10 medium supplemented with 15% horse serum and 2.5% FCS (all from Sigma) with 2 mmol/L glutamine, 100 IU/mL penicillin, and 100 μg/mL streptomycin (37°C, 95% humidity, 5% CO_2 atmosphere incubation).

We used the FGF7 ligand to examine the effect of FGFR2 activation on pituitary cell cycle progression. This FGF was chosen on the basis of its selective binding to FGFR2 (7). One million AtT20 cells were treated with FGF7 (7, 15 ng/mL) or vehicle (as control) for 24 h in the presence of heparin (10 units/mL). Estrogen treatment (17 β-estradiol, 0-3 μmol/L; Sigma) with or without ICI 182780 (10^{-9}-10^{-6} mol/L; Sigma) was done under serum-free conditions in phenol red–free Ham's F-10 medium for 72 h.

For assessment of effect of DNA methylation, cells were treated with freshly prepared 5 and 10 μmol/L of the DNA methyltransferase inhibitor 5-aza-2′-deoxycytidine (aza-CR; Sigma) for 5 d. At 48-h intervals, fresh medium containing the drug was added. For assessment of chromatin histone acetylation, cells were treated with 0.3 and 0.6 μmol/L of the histone deacetylase inhibitor trichostatin A (TSA; Sigma) for 24 h. Each experiment was independently done in three separate dishes in at least three independent experiments.

Cell proliferation assay. Cells were seeded in a 96-well plate and labeled with 3-(4,5-dimethylthiazol-2-yl)-2,5-diphenyltetrazolium bromide (Sigma) as a measure of cell proliferation. Absorbance was measured with an OPTI max microplate reader (Molecular Devices) at 570 nm and reference wavelength of 650 nm.

SiRNA down-regulation of MAGE-A3. Oligonucleotides complementary to a region of the mouse MAGE-A3 (Fig. 4A) were synthesized by Ambion. The forward strand 5′-GUGGACUCCUCUGUCCACAtt-3′ and reverse strand 5′-UGUGGACAGAGGAGUCCACtt-3′ were transfected using Lipofectamine at 200 and 400 pmol concentrations as indicated.

Western blotting. Cells were lysed with radioimmunoprecipitation assay buffer (1% NP40, 0.5% sodium deoxycholate, 0.1% SDS, 100 μg/mL phenylmethylsulfonyl fluoride, aprotinin, and sodium orthovanadate in PBS). Total cell lysates were quantified by the Bio-Rad method. Fifty micrograms of whole lysates were separated on 10% SDS denaturing polyacrylamide gels and transferred onto nylon membrane (Millipore) at 100 V for 1.5 h at room temperature. Blots were incubated with antibodies to p53 (monoclonal, DO-1, 1:1,000; Santa Cruz Biotechnology), the cyclin-dependent kinase inhibitor p21 (monoclonal, 1:1,000; BD Biosciences), and actin (monoclonal, 1:2,000; Sigma) as a loading control. Blocking was achieved in TBS-5% nonfat milk with 0.1% Tween at 4°C overnight, followed by washing with PBS-Tween 20 four times for 10 min each at room temperature and incubated with peroxidase-conjugated goat anti-mouse IgG (1:2,000) for 1 h at room temperature with agitation. Protein bands were visualized by chemiluminescence (Amersham) and band intensities were quantified by Quantity One Software (Bio-Rad).

Immunocytochemistry. AtT20 cell pellets were fixed in formalin and embedded in paraffin for immunohistochemical evaluation of p53 expression after transfection with MAGE-A3 siRNA. Sections of 4-μm thickness were treated with 2% hydrogen peroxide to quench endogenous peroxidase for 30 min and exposed to 5 μg/mL proteinase K for 15 min at room temperature. The sections were extensively washed and exposed to equilibration buffer for 10 min. Each slide was then incubated with anti-p53 antibody (monoclonal, 1:1,000; Santa Cruz Biotechnology) at 4°C overnight. The reaction was visualized with the avidin-biotin method and 3,3′-diaminobenzidine.

RNA extraction and semiquantitative reverse transcription-PCR. Total RNA was isolated from human pituitary tissue using TriZol reagents (Invitrogen Corp.). RNA from AtT20 cells was isolated using RNeasy Mini Kit (Qiagen), combined with optional on-column DNase digestion by RNase-Free DNase Set (Qiagen) according to the manufacturer's instructions to diminish genomic DNA contamination.

Approximately 1.0 μg of total DNase-treated RNA from each sample was used to conduct reverse transcription in a 20-μL volume using TaqMan reverse transcription reagents kit (Applied Biosystems, Inc.). The synthesized cDNA was used for PCR amplification or stored at -20°C for further analysis. Reverse transcription-PCR (RT-PCR) primers were designed to span exons to avoid genomic DNA contamination except in the case of mouse MAGE-A3 where each sample included a reverse transcriptase omission control. The primer sequences and PCR conditions are shown in Table 2. PCR reactions were carried out for 10 min at 95°C followed by 33 or 38 cycles of 30 s at 95°C, 30 s at annealing temperatures, and 30 s at 72°C, followed by a 10-min extension at 72°C. RT-PCR examinations were done on at least three independent occasions.

DNA extraction, bisulfite treatment, and DNA sequencing. Pituitary tissue was digested overnight at 50°C in a buffer containing 50 mmol/L Tris-HCl (pH 8.0), 0.1 mmol/L EDTA (pH 8.0), 0.1 mmol/L NaCl, 1% SDS, and 200 μg/mL proteinase K, followed by phenol/chloroform extraction and ethanol precipitation. DNA was stored at -20°C. One microgram of genomic DNA was bisulfite modified according to the manufacturer's protocol (Chemicon International) and diluted in 25-μL volume. One microliter of modified DNA was used for bisulfite sequencing PCR. Primer sequences and PCR conditions are indicated in Supplementary Table S2. Two rounds of PCR reactions were carried out for bisulfite-sequencing PCR, both for 10 min at 95°C followed by 40 cycles of 30 s at 95°C, 45 s at annealing temperature, and 45 s at 72°C, followed by a 10-min extension at 72°C. Final PCR products were cut from 1.5% agarose gels, extracted, and cloned into the TA cloning system (Invitrogen) for automated sequencing. At least 10 positive clones from each sample were sequenced.

Quantification of DNA methylation. DNA methylation level was measured by combined bisulfite restriction analysis. Briefly, bisulfite-treated DNA was PCR amplified (Table 2) to cover the CpG sites where alternative methylation would be expected to generate multiple *Bst*UI products. Ten micrograms of purified bisulfite PCR products were incubated in a 15-μL volume reaction with 5 units of *Bst*UI (New England Biolabs) overnight at 60°C. Restriction digestion products were separated on 2.5% agarose gels, followed by UV exposure. Experiments were done on three independent occasions, following which product intensities were quantified by scanning densitometry (Quantity One Software, Bio-Rad). The digested band (methylated)

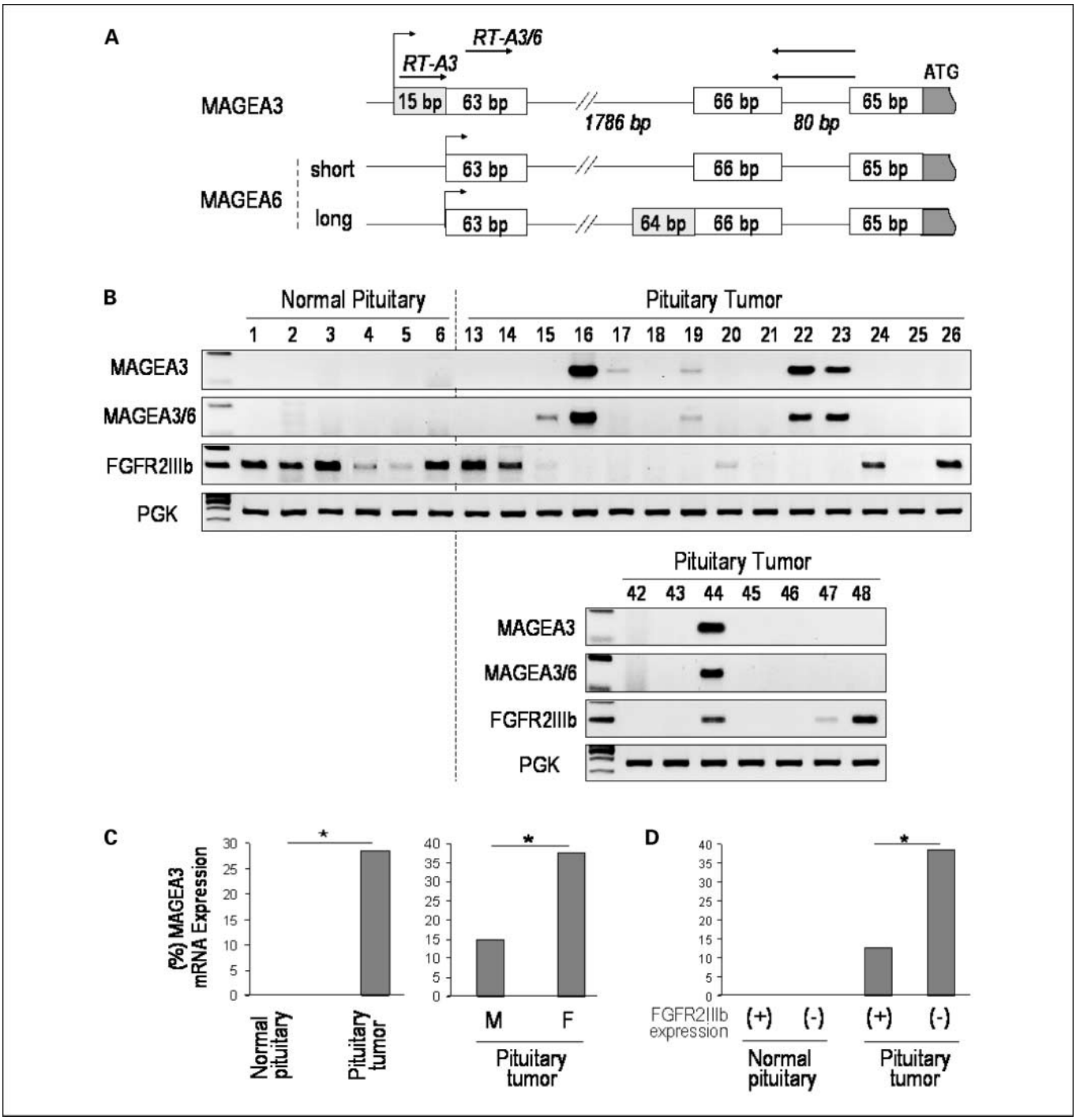

Fig. 1. MAGE-A3 is expressed in human pituitary tumors. *A,* a RT-PCR approach for the detection of MAGE-A3 and for distinction from the short and long isoforms of the related family member MAGE-A6. Arrows, location of forward and reverse primers. *B,* MAGE-A3–specific primers identify transcripts in pituitary tumor samples but not in normal pituitary tissue. Conversely, FGFR2-IIIb, a putative regulator of MAGE-A3, is expressed in normal pituitary but frequently down-regulated in tumorous samples. All MAGE-A3–containing samples also yielded products using primers for the common MAGE-A3/6 region. Amplification of the human *PGK* gene was used as a reference. See Table 1 for detailed description of samples examined. *C,* summary of frequency of MAGE-A3 expression in normal and pituitary tumor samples (*left*) and in male (*M*) and female (*F*) subjects (*right*). *, $P < 0.005$, Wilcoxon two-sample test. *D,* relationship between MAGE-A3 and FGFR2-IIIb expression in normal and pituitary tumor specimens. *, $P < 0.005$, comparing MAGE-A3 expression in FGFR2-IIIb–positive (+) and FGFR2-IIIb–negative (-) samples (Wilcoxon two-sample test).

intensity divided by all products (methylated + unmethylated) yielded the methylation level (% ratio).

Chromatin immunoprecipitation assays. The chromatin immunoprecipitation assay was done in accordance with the manufacturer's recommendations (UBI) and as previously described (17). Briefly, histone was cross-linked to DNA by the direct addition of 37% formaldehyde, and cells were washed with cold PBS containing protease inhibitors before lysis. Lysates were sonicated to shear DNA lengths of 200 to 1,000 bp. After centrifugation, cell suspensions were further diluted and 20 μL of lysate from each sample were used to monitor the amount of DNA present (input DNA) for PCR detection. The rest of the lysate was cleared with salmon sperm DNA/protein G-agarose beads.

Immunoprecipitation was done with anti–acetyl-histone 3 and anti–dimethyl-histone 3 (Lys9) antibodies (both from UBI) overnight at 4°C with agitation. The latter was selected on the basis of its specific contribution to epigenetic silencing and sensitivity to aza-CR treatment (25). Negative controls included omission of antibody or use of an anti-IgG antibody. For PCR analysis, the histone-DNA cross-links of eluates were reversed at 65°C, and the immunocomplexes were digested with proteinase K for 1 h at 50°C, and DNA was finally purified by phenol extraction and used for PCR amplification. PCR primers and conditions are shown in Table 2. Experiments were done on three independent occasions and quantified by scanning densitometry (Quantity One Software, Bio-Rad).

Statistical analyses. Data were analyzed using the SAS software system. The values presented represent the mean ± SD obtained from three independent experiments. Comparisons between the means were tested using the Wilcoxon two-sample test with a significance level assigned at a threshold of <0.05.

Results

MAGE-A3 is expressed in human pituitary tumors. We have previously reported that FGFR2 is abundantly expressed in the normal pituitary gland but frequently down-regulated in

Table 1. List of primary human pituitary samples

Case no.	Sex	Pathologic diagnosis	FGFR2		MAGE-A3	
			mRNA expression	DNA methylation	mRNA expression	Methylation level (%)
mRNA analyses						
1	M	Normal	+		-	
2	F	Normal	+		-	
3	F	Normal	+		-	
4	M	Normal	+		-	
5	M	Normal	+		-	
6	F	Normal	+		-	
13	M	Mixed lactotroph-somatotroph adenoma	+		-	
14	M	Oncocytoma	+		-	
15	F	Corticotroph adenoma	-		-	
16	F	Silent subtype 3 adenoma	-		+	
17	M	Lactotroph adenoma (sparsely granulated)	-		+	
18	M	Somatotroph adenoma (densely granulate)	-		-	
19	F	Lactotroph adenoma	-		+	
20	F	Lactotroph adenoma	+		-	
21	F	Gonadotroph adenoma	-		-	
22	M	Somatotroph adenoma (densely granulated)	-		+	
23	F	Somatotroph adenoma (densely granulated)	-		+	
24	F	Corticotroph adenoma	+		-	
25	M	Somatotroph adenoma (sparsely granulated)	-		-	
26	F	Somatotroph adenoma (sparsely granulated)	+		-	
DNA analyses						
7	F	Normal		-		61
8	M	Normal		-		98
9	M	Normal		-		94
10	F	Normal		+		99
11	M	Normal		-		93
12	F	Normal		-		99
27	F	Acidophil stem cell adenoma		+		20
28	M	Gonadotroph adenoma		+		73
29	F	Gonadotroph adenoma		-		13
30	F	Lactotroph adenoma (sparsely granulated)		+		29
31	M	Lactotroph adenoma (sparsely granulated)		-		86
32	F	Somatotroph adenoma (sparsely granulated)		+		5
33	M	Lactotroph adenoma (sparsely granulated)		+		42
34	M	Somatotroph adenoma (sparsely granulated)		-		8
35	M	Gonadotroph adenoma		+		79
36	M	Somatotroph adenoma (densely granulated)		+		62
37	F	Lactotroph adenoma		-		12
38	F	Corticotroph adenoma		-		5
39	F	Corticotroph adenoma		-		2
40	M	Lactotroph adenoma (sparsely granulated)		+		61
41	M	Mixed lactotroph-somatotroph adenoma		-		45
mRNA and DNA analyses						
42	M	Lactotroph adenoma (sparsely granulated)	-	+	-	58
43	M	Oncocytic adenoma	-	+	-	90
44	M	Somatotroph adenoma (sparsely granulated)	+	-	+	11
45	M	Gonadotroph adenoma	-	+	-	15
46	M	Oncocytic adenoma	-	+	-	23
47	M	Oncocytic adenoma	+	-	-	28
48	M	Gonadotroph adenoma	+	-	-	63

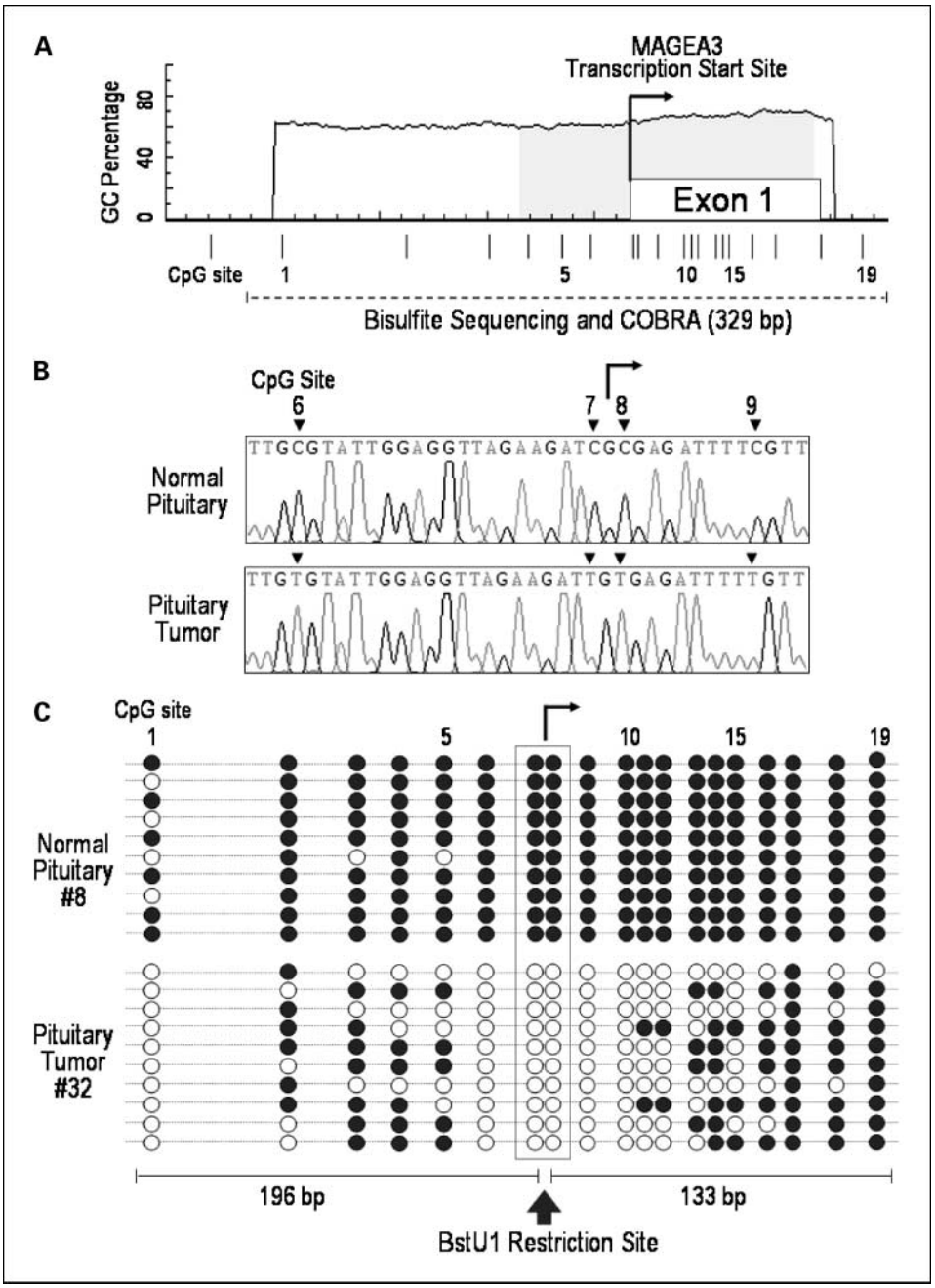

Fig. 2. Detection of MAGE-A3 promoter methylation in normal and tumorous pituitary tissue. *A,* the human MAGE-A3 promoter region from -365 to +119 encompassing the 5′ untranslated region and exon 1 contains a CpG island where aberrant CG sites are denoted by vertical bars below the graph. Square arrow, transcription start site, which is specifically hypomethylated in pituitary tumors. Dotted line, the region examined by bisulfite DNA sequencing. Sequence numbering follows GenBank accession NC.000023. *B,* bisulfite sequencing was done covering the region from -198 to +131, which includes 19 CpG dinucleotide sites. Square arrow, transcription start site, which is also situated within a *Bst*UI restriction site. *C,* a string-on-a-bead representation of independently sequenced clones for samples shown in *B* is depicted. Results of bisulfite sequencing reveal extensive methylation (*closed circles*) of the gene promoter in a normal human pituitary specimen. In contrast, a representative pituitary tumor shows hypomethylation (*open circles*) surrounding the transcription start site. See Table 1 for detailed description of samples examined.

human pituitary tumors (15, 20). Further, we have shown that FGFR2 can potently mediate the down-regulation of the MAGE-A3/A6 cancer-testis antigen (22). Thus, we tested the hypothesis that loss of FGFR2 in human pituitary tumors would lead to the ectopic expression of MAGE-A3. To specifically address this question, we used an RT-PCR approach to determine if MAGE-A3 and/or its closely related family member MAGE-A6 is expressed in human pituitary tumors. Using primers to distinguish MAGE-A3 from MAGE-A3/6 (Fig. 1A), we identified the expression of MAGE-A3 in 6 of 21 (29%) human pituitary tumors (Fig. 1B). In contrast, none of six normal human pituitary samples had detectable expression of MAGE-A3 or MAGE-A3/A6 ($P < 0.001$). Moreover, FGFR2-IIIb was expressed in normal pituitary specimens but was down-regulated in the majority of pituitary tumors (Fig. 1B and C). A summary of the RT-PCR analyses of all samples examined for MAGE-A3 and FGFR2 and their pathologic characterization are shown in Table 1. Note that MAGE-A3 expression was more frequent in FGFR2-negative tumors (5 of 13, 39%) than in FGFR2-positive tumors (1 of 8, 12%; Fig. 1D). Moreover, MAGE-A3 expression was more than twice as frequent in female subjects (38%) as in males (15%; Fig. 1C).

The MAGE-A3 promoter is preferentially hypomethylated in pituitary tumors. To identify a potential mechanism for the expression of MAGE-A3 in pituitary tumors and its extinction in the normal gland, we examined the methylation state of the MAGE-A3 promoter in both tissues. The human MAGE-A3 promoter region from -365 to +119 encompassing the

5′ untranslated region and exon 1 contains a CpG, island as indicated in Fig. 2A. Thus, we used DNA sequencing following bisulfite treatment to cover the region from -198 to +131, which includes 19 CpG dinucleotide sites. As shown in Fig. 2B and C, we found evidence of extensive *MAGE-A3* gene promoter methylation in normal human pituitary specimens. In contrast, a pituitary tumor showed hypomethylation at the same CpG sites particularly surrounding the transcription start site (Fig. 2B and C). This prompted us to do a more extensive assessment to compare the degrees of MAGE-A3 promoter methylation in normal human and neoplastic pituitary specimens using a combined bisulfite restriction analysis approach (Fig. 3A). As shown in Fig. 3B, there was more extensive MAGE-A3 methylation in normal pituitary samples compared with neoplastic pituitaries. Because MAGE-A3 is positioned on the X chromosome (26), we examined a putative relationship between MAGE-A3 methylation and gender (Fig. 3C). This showed a significantly higher frequency of promoter

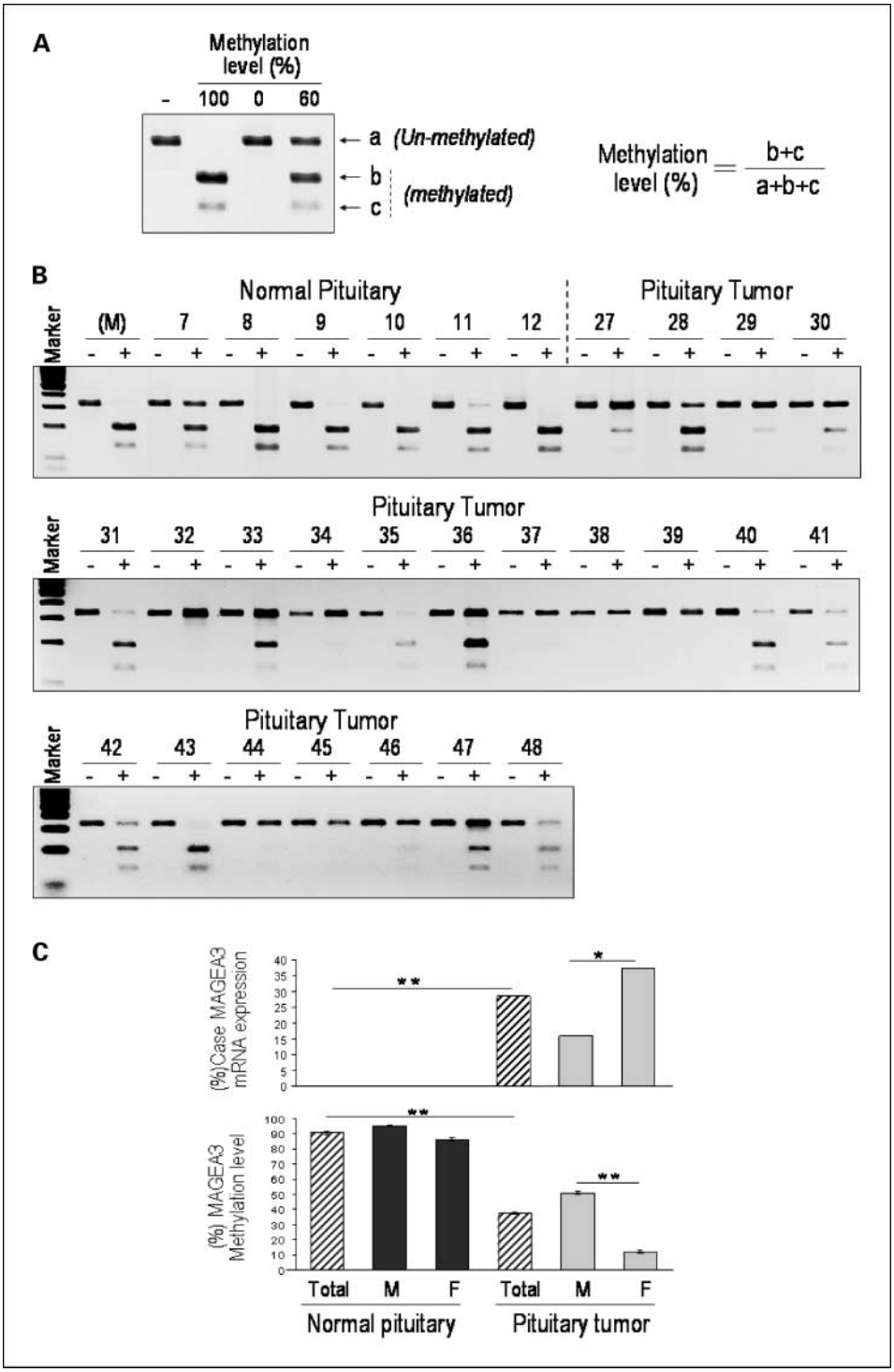

Fig. 3. Comparison of the extent of MAGE-A3 promoter methylation in normal and tumorous human pituitary tissue. *A,* combined bisulfite restriction analysis was done as an index of the degree of MAGE-A3 promoter methylation. The percent of methylation was derived from the ratio of densitometric methylated products ($b + c$) compared with the total sum of the products ($a + b + c$) as indicated. *B,* combined bisulfite restriction analysis of normal and pituitary tumor tissue as detailed in Table 2. - and +, without and with *Bst*UI digestion, respectively. M, a universal human DNA methylation – positive control. Individual sample examination reveals more extensive methylation in normal tissue compared with pituitary tumor samples. *C,* summary of frequency of MAGE-A3 expression (*top*) and promoter methylation (*bottom*) in normal and neoplastic pituitary tissues. M, samples derived from male subjects; F, samples derived from females. *, $P < 0.01$; **, $P < 0.001$.

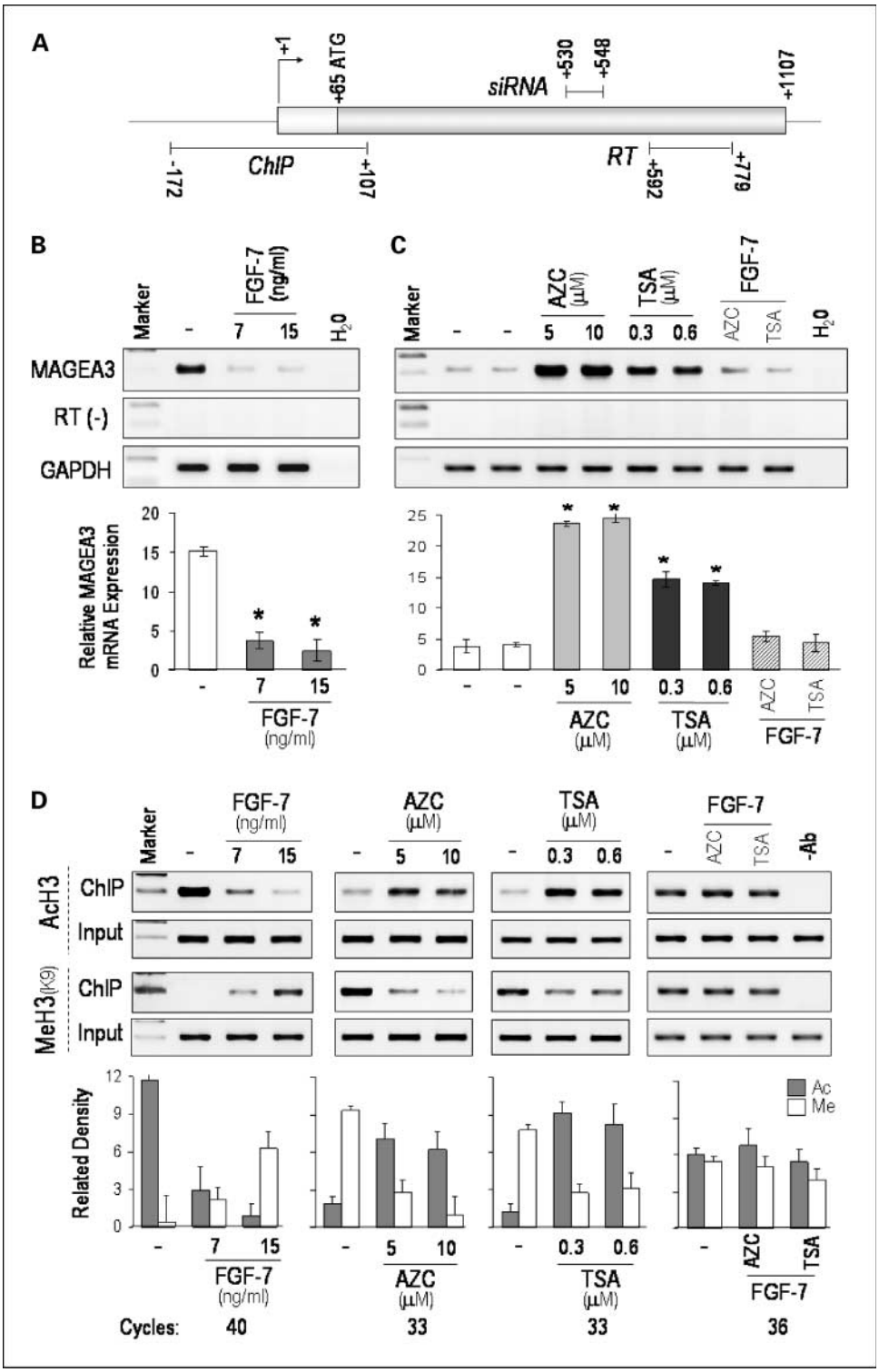

Fig. 4. MAGE-A3 is subject to epigenetic control through FGFR2 signaling in mouse pituitary AtT20 cells. *A,* the mouse MAGE-A3 promoter region encompassing the 5′ untranslated region and the single exon is indicated. The square arrow represents the transcription start site. The underlined regions correspond to the sites examined by chromatin immunoprecipitation (*ChIP*) and RT-PCR (*RT*). Numbering for genomic and cDNA sequences follows GenBank accession nos. NC000086 and BC119064.1, respectively. *B,* AtT20 pituitary corticotroph cells were stimulated with the FGFR2-IIIb – selective FGF7 ligand and examined by RT-PCR following 38 cycles as detailed in Materials and Methods, or treated with the methylation inhibitor aza-CR (*AZC*) or with the histone deacetylation inhibitor TSA and examined by RT-PCR following 33 cycles (*C*). MAGE-A3 mRNA expression levels are significantly enhanced following aza-CR or TSA treatment. Conversely, treatment with FGF7 results in MAGE-A3 down-regulation. *D,* chromatin immunoprecipitation analysis covering the mouse MAGE-A3 5′ upstream transcription start region as shown in a panel using anti – methyl-histone H3-Lys9 (*MeH3-K9*) and anti – acetyl-histone 3 (*AcH3*) antibodies as indicated. Note the deacetylating effect of FGF7 on histone 3 with concomitant enhancement of histone methylation. In contrast, aza-Cr or TSA treatment displays opposing actions on these histone modifications.

methylation in tumors from male patients (51%) compared with tumors from female patients (12%; $P < 0.002$). Consistent with the finding that MAGE-A3 was not expressed in the normal pituitary, there was no difference between the degrees of MAGE-A3 promoter methylation in normal male and female subjects (Fig. 3C).

Methylation and FGFR2 regulation of MAGE-A3 in mouse pituitary AtT20 cells. To determine whether FGFR2 can modulate MAGE-A3 expression in pituitary cells, we examined the effect of the FGFR2-IIIb-selective ligand FGF7 on mouse pituitary AtT20 cells. RT-PCR was done using the mouse MAGE-A3 primers shown in Fig. 4A and listed in Table 2. FGF7 treatment resulted in potent reduction of MAGE-A3 expression (Fig. 4B). To determine if MAGE-A3 is regulated through a methylation-sensitive manner in this system, we examined the effect of the methylation inhibitor aza-CR or the histone

Table 2. List of primers and PCR conditions

Primer	Forward (5′-3′)	Reverse (5′-3′)	T_m (°C)	Product (bp)
RT-PCR				
Human MAGE-A3	gagattctcgccctgagc	ccactggcagatcttctccttc	57	152
Human MAGE-A3/6	caacgagcgacggcctgac	ccactggcagatcttctccttc	59	134, 198
Human FGFR2 IIIb	agtgctggctctgttcaatgtg	ggcgattaagaagacccctatg	58	202
Human p53	actaagcgagcactgcccaac	cctcattcagctctcggaacatc	60	130
Human p21	tggagactctcagggtcgaaaac	caggactgcaggcttcctgtg	60	121
Human PGK	gctgacaagtttgatgagaat	aggactttaccttccaggagc	58	338
Mouse MAGE-A3	gatgactgatgtccagggtatgc	gcacaaactcctcagagatgagc	60	188
Mouse p53	cacagcgtggtggtaccttatg	aaggttcccactggagtcttcc	59	153
Mouse GAPDH	atcactgccacccagaagact	catgccagtgagcttcccgtt	56	152
Mouse ERα	aatgatgggcttattgaccaacc	cgagaccaatcatcagaatctcc	59	152
Mouse ERβ	gtctgcagtgattatgcatctgg	agcttttacgccggttcttgtc	59	151
Human bisulfite sequencing and COBRA				
MAGE-A3 BS (outer)	gtattaattttaggattttgagggatg	ttaaaaccctctatctaaaataaaacc	56	392
MAGE-A3 BS (inner)	gattttattaggatttatagttttagg	ttaaaaccctctatctaaaataaaacc	53	329
Chromatin immunopreciptation				
Mouse MAGE-A3	actccaaatggcagggtaacttc	tctcttcgaggttgcagtattgg	58	279
Mouse p53	ggcggtccacttacgataaaaac	actcctggcacaaagctggatag	58	262

Abbreviations: ER, estrogen receptor; COBRA, combined bisulfite restriction analysis.

deacetylation inhibitor TSA, followed by RT-PCR examination (Fig. 4C). This approach identified robust up-regulation of MAGE-A3 in response to either treatment, which, given the lack of a mouse 5′ CpG island, suggested the potential role of histone modifications in the control of this gene. Furthermore, FGF7 treatment abrogated the effect of aza-CR or TSA on MAGE-A3 expression (Fig. 4C). Thus, to further clarify the epigenetic regulation of MAGE-A3, we examined histone modifications associated with the 5′ upstream transcription start region using a chromatin immunoprecipitation approach as shown in Fig. 4A. This revealed the ability of FGF7-mediated FGFR2-IIIb signaling to enhance histone Lys9 methylation with concomitant deacetylation of histone 3 tails (Fig. 4D). In contrast, aza-CR or TSA treatment resulted in opposing actions on these histone modifications with diminished methylation and enhanced acetylation, consistent with the observed effects on *MAGE-A3* gene regulation (Fig. 4C). Furthermore, FGF7 abrogated the effect of aza-CR or TSA treatment on histone modifications associated with the MAGE-A3 promoter (Fig. 4D).

MAGE-A3 is sensitive to estrogen induction through histone modifications. To determine why MAGE-A3 is more frequently expressed in tumors from female subjects, we examined the effect of estrogen treatment on this putative oncogene. As shown in Fig. 5, estradiol treatment resulted in a dose-dependent induction of MAGE-A3 mRNA levels (Fig. 5A). That the effect of estradiol was mediated through the estrogen receptor was supported by the detection of estrogen receptor β in these cells (Fig. 5B, *left*). Moreover, the use of the estrogen receptor inhibitor ICI 182780 resulted in a dose-dependent inhibition of estradiol action on MAGE-A3 (Fig. 5B, *right*). Furthermore, FGF7 abrogated the effect of estradiol on MAGE-A3 mRNA expression (Fig. 5C). Consistent with the effect of estradiol on MAGE-A3, treatment with this steroid resulted in enhanced acetylation on histone 3 sites with corresponding decline in methylation of the MAGE-A3 promoter (Fig. 5D). Moreover, FGF7 abrogated the effect of estradiol on these histone modifications associated with the MAGE-A3 promoter (Fig. 5D).

MAGE-A3 targets transcriptional regulation of p53 in pituitary cells. Emerging data suggest potential involvement of MAGE family proteins in modulating cell survival through opposing actions on p53. In particular, MAGE-A2 was recently shown to repress p53 (27). Thus, we examined the effect of MAGE-A3 down-regulation on p53. Reduction of MAGE-A3 using siRNA resulted in pronounced induction of p53 mRNA (Fig. 6A) and protein (Fig. 6B) levels. Consistent with the effect on p53, down-regulation of MAGE-A3 resulted in up-regulation of the cyclin-dependent kinase inhibitor p21 (Fig. 6B). Forced down-regulation of MAGE-A3 resulted in enhanced acetylation of histone 3 associated with the p53 promoter with concomitant reduction in histone methylation (Fig. 6C). We also show that reduction of MAGE-A3 results in reduced cell proliferation (59.6 ± 0.01% of control, 20 nmol/L siRNA; 51.8 ± 0.01% of control, 40 nmol/L siRNA) as indicated by 3-(4,5-dimethylthiazol-2-yl)-2,5-diphenyltetrazolium bromide assay. Finally, we show that primary human pituitary tumors (as described in Fig. 1) show diminished p53 and p21 expression as compared with normal tissue (Fig. 6D). Taken together, these data provide evidence for a network of histone modifications in the control not only of MAGE-A3 itself but also of at least one of its putative targets, p53.

Discussion

We describe here the initial characterization of MAGE-A3 in human and mouse pituitary tumor cells. We show that MAGE-A3 is reciprocally expressed in tumors where FGFR2-IIIb is absent. These data validate gene profiling evidence that the putative oncogene MAGE-A3 is indeed a target of FGFR2 action (22). We also show here, for the first time, that MAGE-A3 expression is intimately linked with the frequency and degree of promoter hypomethylation, particularly in tumors from female subjects. This observation is consistent with the induction of MAGE-A3 by estrogen through histone modification. This latter action abrogates the effect of FGFR2-IIIb, highlighting MAGE-A3 as a point of signaling integration between opposing forces (Fig. 7).

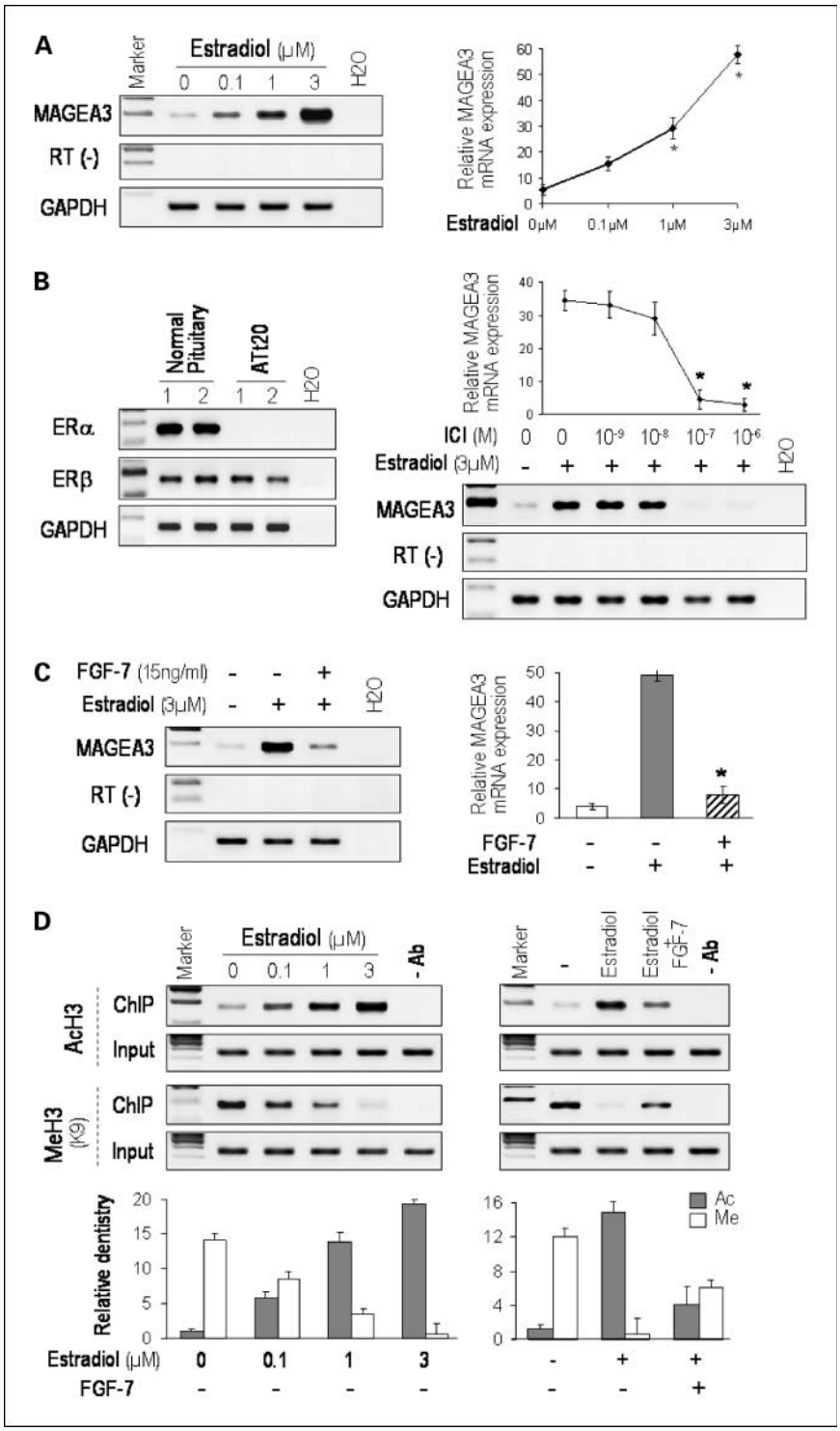

Fig. 5. Estrogen induces MAGE-A3 expression through histone modifications in mouse pituitary AtT20 cells. *A,* AtT20 mouse pituitary cells were treated with increasing doses of estradiol alone under serum-free conditions as detailed in Materials and Methods. Total RNA was examined by RT-PCR using primers as shown in Fig. 4A. Negative controls omitted reverse transcriptase [*RT* (-)] or replaced sample with water (H_2O). The housekeeping gene glyceraldehyde-3-phosphate dehydrogenase (*GAPDH*) was used as a loading control for semiquantitative comparison. Right, points, mean from three independent experiments; bars, SD. *, $P < 0.01$, compared with vehicle control. *B,* detection of estrogen receptor (*ER*) isoforms α and β in normal and neoplastic AtT20 pituitary cells by RT-PCR (*left*). Cells treated as in *A* were also examined in the absence or presence of increasing concentrations of the estrogen receptor inhibitor ICI 182780 (*ICI*; *right*). The magnitude of attenuation by ICI 182780 is shown by the graph immediately above. *C,* cells treated as in *A* were also examined in the absence or presence of the FGFR2-selective ligand FGF7. RT-PCR examination reveals an attenuating effect of FGF7 on estrogen-mediated MAGE-A3. Right, columns, quantitative mean values; bars, SD. *D,* the effect of FGF7 on estradiol-mediated MAGE-A3 activation was also examined by chromatin immunoprecipitation assay as depicted in Fig. 4A, using anti – dimethyl-histone H3-Lys9 (*MeH3-K9*) and anti – acetyl-histone 3 antibodies as indicated. Note the dose-dependent enhancement by estradiol on histone 3 acetylation with corresponding decline in methylation associated with the MAGE-A3 promoter. Note also the ability of FGF7 to abrogate the effect of estradiol on histone changes, consistent with the opposing actions of these two ligands on these modifications. Quantitative measurements of the independent and combined effects of FGF7 and estradiol are shown in the bar graph immediately below.

We have previously noted the presence of both FGFR2-IIIb and FGFR2-IIIc isoforms in normal human pituitary cells (15). Pharmacologic methylation inhibition resulted in mainly FGFR2-IIIb reexpression with minimal effect on the IIIc isoform in pituitary cells (20). Similar findings of FGFR2-IIIb isoform silencing have previously been noted in prostate cancer (28) and in transitional cell carcinomas of the bladder (29, 30). Reexpression of FGFR2-IIIb results in potent tumor growth inhibition with enhanced apoptosis (31). This effect has been ascribed to the ability of FGFR2-IIIb to sequester the FGFR substrate 2 (32), diverting it away from other competing FGFR signal (22). Consistent with this model, FGFR2-IIIb activation using its selective ligand FGF7 results in diminished pituitary tumor cell cycle progression (20). This effect was recapitulated here through down-regulation of MAGE-A3, which resulted in p53 and p21 induction, providing further functional evidence implicating MAGE-A3 as an important downstream mediator of FGFR2-IIIb signaling.

MAGE-A3 and *MAGE-A6* genes are members of the MAGE-I family that includes the MAGE-A, MAGE-B, and MAGE-C subfamilies (33). The MAGE-I family consists of a number of X chromosome clustered genes, which are expressed mainly in testicular germ cells, placenta, and a variety of malignant tumors, resulting in their designation as cancer-testis antigens (33–37). Our current data are the first to describe the presence of MAGE-A3 transcripts in pituitary tumors. Further, we show that MAGE-A3 can target the transcriptional regulation of p53, consistent with one previous report implicating MAGE-A2 in p53 regulation (27). Moreover, MAGE-A3 down-regulation resulted in p53 and p21 accumulation, consistent with the putative oncogenic functions of this cancer antigen. It is worthy to note that whereas p53 is not intragenically mutated in pituitary tumors, variable levels of p53 protein accumulation have been reported in these neoplasms (38). Our current findings therefore suggest that MAGE-A3 may represent an important candidate gene responsible for p53 dysregulation in pituitary tumors.

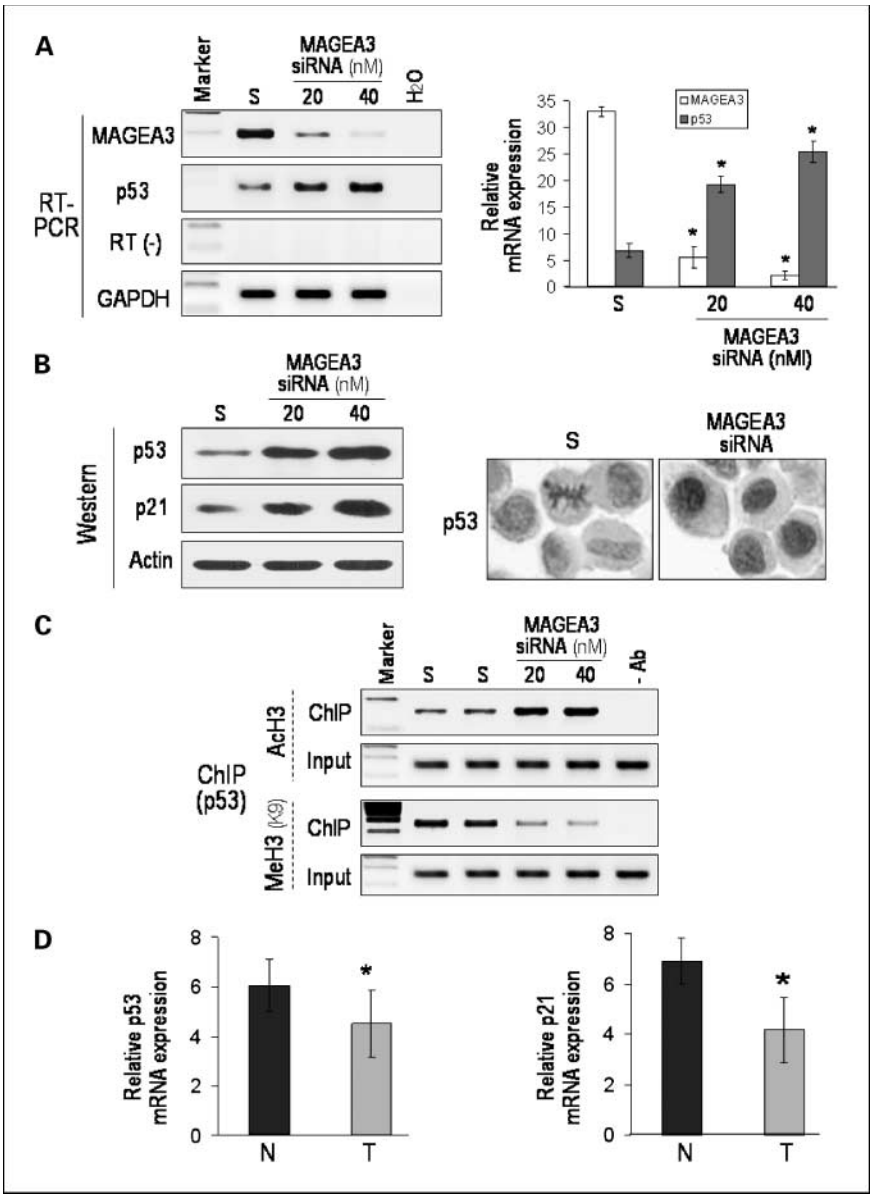

Fig. 6. Forced down-regulation of MAGE-A3 promotes p53 transcriptional induction. *A,* AtT20 mouse pituitary cells were transfected with siRNA directed against MAGE-A3 or with a scrambled (*S*) control. RNA was subjected to RT-PCR examination for p53 or MAGE-A3 (*left*). *B,* Western blotting examination confirms that MAGE-A3 down-regulation results in accumulation of p53 and consequently its downstream target p21. Immunocytochemistry of corresponding cell pellets (*right*) show increased p53 nuclear residence. *C,* AtT20 cells down-regulated for MAGE-A3 as in *A* were examined by chromatin immunoprecipitation assay covering the mouse p53 promoter. Note the enhancement of histone 3 acetylation with corresponding decline in methylation associated with the p53 promoter in response to down-regulation of MAGE-A3. *D,* relationship between p53 (*left*) and p21 (*right*) mRNA expression in normal (*N*) and primary pituitary tumor (*T*) samples as described in Fig. 1.

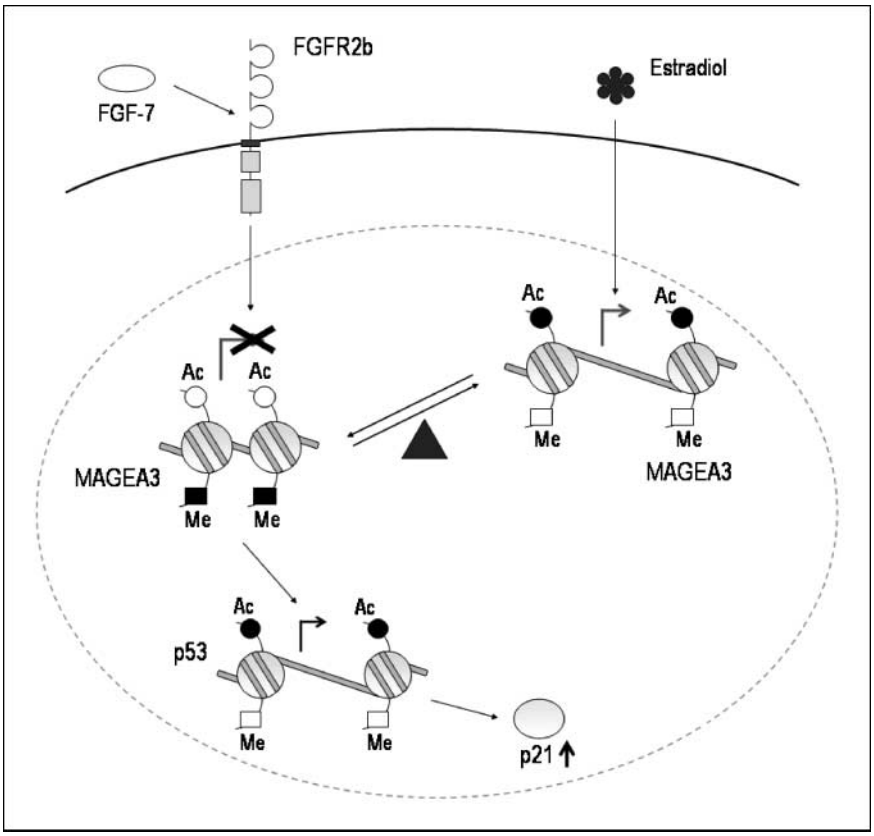

Fig. 7. Schematic diagram outlining the dual opposing actions of FGF7/FGFR2-IIIb and estradiol on MAGE-A3. The balance represents the converging actions of the two ligand systems on acetylation (*Ac*) and methylation (*Me*) modifications of histone tails associated with the MAGE-A3 promoter. Down-regulation of MAGE-A3 results in enhanced acetylation and diminished methylation leading to p53 induction, protein accumulation, and, consequently, increased p21. Closed circles or squares, enhanced modification; open circles, diminishing effect.

Our data also point to several putative mechanisms underlying the loss and gain of expression of the MAGE-A3 in normal and neoplastic pituitary cells, respectively. Previous reports implicated CpG methylation status in the 5′ region of MAGE-A genes in the process of regulation (39, 40). In line with this prediction, we found that the MAGE-A3 promoter is heavily methylated in normal human pituitary cells, resulting in lack of expression in this tissue. In contrast, we found the MAGE-A3 promoter to be hypomethylated in pituitary tumors. These findings provide further evidence supporting epigenetic regulation through DNA methylation as a mechanism behind the ectopic expression of putative oncogenes such as MAGE-A3 in human pituitary tumors.

Our current study also shows that MAGE-A3 is generally down-regulated where FGFR2-IIIb is expressed. These findings and our previous data (22) suggest that FGFR signaling can epigenetically modulate *MAGE-A3* gene expression, providing evidence for an interregulatory loop. Taken together, the current evidence provides further validation for the role of FGFR2-IIIb signaling, a putative tumor-retarding factor (20, 31), in the epigenetic modifications leading to MAGE-A3 down-regulation. Conversely, estrogen treatment, a potent stimulator of pituitary tumor progression (2, 41), was associated with MAGE-A3 induction. This latter effect was shown to also occur through histone modifications.

An emerging theme from studies of human pituitary tumors is altered epigenetic control rather than intragenic mutations, loss of heterozygosity, or gene rearrangements (42). For example, consistent with its well-recognized effect on pituitary neoplasia in genetically deficient mice (43), the Rb tumor suppressor gene is principally silenced through CpG island methylation in neoplastic human pituitary cells (44–46). No inactivating mutations have been identified within the Rb1 promoter region in pituitary tumors that fail to express the protein (47). Similarly, mice lacking $p27^{kip1}$ have an increased propensity to develop multiorgan neoplasia, including pituitary tumors (48), and protein levels of this cyclin-dependent kinase inhibitor are reduced in human pituitary adenomas; however, the $p27^{kip1}$ gene is not mutated (49, 50). Expression of GADD45γ, a member of a growth arrest and DNA damage-inducible gene family, is diminished in pituitary tumors (51) through CpG island promoter methylation (52). More recently, the Ras association domain family 1A gene (RASSF1A), originally cloned from the lung tumor locus at 3p21.3, is frequently inactivated through promoter hypermethylation in pituitary tumors (53). MEG3, a human homologue of the mouse maternally imprinted *Gtl2* gene, is also down-regulated in human pituitary tumors through 5′ promoter hypermethylation (54). MAGE-A3 is another X chromosome–linked gene that has been shown to be epigenetically imprinted (26). Consistent with this prediction, we identified a greater frequency of MAGE-A3 expression and promoter hypomethylation in pituitary tumors as a group and more so in female subjects. Interestingly, estrogen potently up-regulates MAGE-A3, and consistent with the sensitivity of the MAGE-A3 promoter to histone modifications, estrogen induction of MAGE-A3 was associated with enhanced histone acetylation and concomitant reduction in histone methylation. More significantly, we show that the effects of estrogen and FGF7/FGFR2-IIIb are precisely reciprocal in modifying histones associated with MAGE-A3.

In summary, our data identify a reciprocal profile of FGFR2-IIIb and MAGE-A3 expression in the normal and neoplastic pituitary. Whereas FGFR2-IIIb plays a growth-inhibitory tumor-suppressive role (31), MAGE-A3 is considered to have growth-promoting oncogenic functions (27, 55). Our current data highlight MAGE-A3 as a novel downstream target of FGFR2-IIIb. They also point to the significance of DNA hypomethylation as well as histone modifications in the ectopic expression of putative oncogenic signals. Given the well-appreciated role of hypermethylation in pituitary tumors, our findings underscore the complex network of epigenetic changes in the control over the balance of signals with opposing functions.

Acknowledgments

We thank Kelvin So for technical assistance.

References

1. Asa SL, Ezzat S. The cytogenesis and pathogenesis of pituitary adenomas. Endocr Rev 1998;19:798–827.
2. Asa SL, Ezzat S. The pathogenesis of pituitary tumours. Nat Rev Cancer 2002;2:836–49.
3. Treier M, Gleiberman AS, O'Connell SM, et al. Multi-step signaling requirements for pituitary organogenesis *in vivo*. Genes Dev 1998;12:1691–704.
4. Paez-Pereda M, Giacomini D, Refojo D, et al. Involvement of bone morphogenetic protein 4 (BMP-4) in pituitary prolactinoma pathogenesis through a Smad/estrogen receptor crosstalk. Proc Natl Acad Sci U S A 2003;100:1034–9.
5. Itoh N, Ornitz DM. Evolution of the Fgf and Fgfr gene families. Trends Genet 2004;20:563–9.
6. Ornitz DM, Zu J, Colvin JS, et al. Receptor specificity of the fibroblast growth factor family. J Biol Chem 1996;271:15292–7.
7. Luo Y, Ye S, Kan M, McKeehan WL. Structural specificity in a FGF7-affinity purified heparin octasaccharide required for formation of a complex with FGF7 and FGFR2IIIb. J Cell Biochem 2006;97:1241–58.
8. Thisse B, Thisse C, Weston JA. Novel FGF receptor (Z-FGFR4) is dynamically expressed in mesoderm and neurectoderm during early zebrafish embryogenesis. Dev Dyn 1995;203:377–91.
9. Thisse B, Thisse C. Functions and regulations of fibroblast growth factor signaling during embryonic development. Dev Biol 2005;287:390–402.
10. Baraniak AP, Lasda EL, Wagner EJ, Garcia-Blanco MA. A stem structure in fibroblast growth factor receptor 2 transcripts mediates cell-type-specific splicing by approximating intronic control elements. Mol Cell Biol 2003;23:9327–37.
11. De Moerlooze L, Spencer-Dene B, Revest J, Hajihosseini M, Rosewell I, Dickson C. An important role for the IIIb isoform of fibroblast growth factor receptor 2 (FGFR2) in mesenchymal-epithelial signalling during mouse organogenesis. Development 2000;127:483–92.
12. Celli G, LaRochelle WJ, Mackem S, Sharp R, Merlino G. Soluble dominant-negative receptor uncovers essential roles for fibroblast growth factors in multi-organ induction and patterning. EMBO J 1998;17:1642–55.
13. Ezzat S, Smyth HS, Ramyar L, Asa SL. Heterogeneous *in vivo* and *in vitro* expression of basic fibroblast growth factor by human pituitary adenomas. J Clin Endocrinol Metab 1995;80:878–84.
14. Asa SL, Ramyar L, Murphy PR, Li AW, Ezzat S. The endogenous fibroblast growth factor-2 antisense gene product regulates pituitary cell growth and hormone production. Mol Endocrinol 2001;15:589–99.
15. Abbass SAA, Asa SL, Ezzat S. Altered expression of fibroblast growth factor receptors in human pituitary adenomas. J Clin Endocrinol Metab 1997;82:1160–6.
16. Ezzat S, Zheng L, Zhu XF, Wu GE, Asa SL. Targeted expression of a human pituitary tumor-derived isoform of FGF receptor-4 recapitulates pituitary tumorigenesis. J Clin Invest 2002;109:69–78.
17. Ezzat S, Yu S, Asa SL. Ikaros isoforms in human pituitary tumors: distinct localization, histone acetylation, and activation of the 5′ fibroblast growth factor receptor-4 promoter. Am J Pathol 2003;163:1177–84.
18. Yu S, Asa SL, Weigel RJ, Ezzat S. Pituitary tumor AP-2α recognizes a cryptic promoter in intron 4 of fibroblast growth factor receptor 4. J Biol Chem 2003;278:19597–602.
19. Ezzat S, Zheng L, Asa SL. Pituitary tumor-derived fibroblast growth factor receptor 4 isoform disrupts neural cell-adhesion molecule/N-cadherin signaling to diminish cell adhesiveness: a mechanism underlying pituitary neoplasia. Mol Endocrinol 2004;18:2543–52.
20. Zhu X, Lee K, Asa SL, Ezzat S. Epigenetic silencing through DNA and histone methylation of fibroblast growth factor receptor 2 in neoplastic pituitary cells. Am J Pathol 2007;170:1618–28.
21. Alexander JM. Tumor suppressor loss in pituitary tumors. Brain Pathol 2001;11:342–55.
22. Kondo T, Zhu X, Asa SL, Ezzat S. The cancer/testis antigen MAGE-A3/6 is a novel target of FGFR2-IIIb through histone H3 modifications in thyroid cancer. Clin Cancer Res 2007;13:4713–20.
23. Asa SL. Tumors of the Pituitary Gland. Third Series [Fascicle 22]. In: Rosai J, editor. Atlas of tumor pathology. Washington (DC): Armed Forces Institute of Pathology; 1998.
24. DeLellis RA, Lloyd RV, Heitz PU, Eng C. Tumours of endocrine organs. In: Kleihues P, editor. World Health Organization classification of tumours. Lyons: IARC; 2004.
25. Wozniak RJ, Klimecki WT, Lau SS, Feinstein Y, Futscher BW. 5-Aza-2′-deoxycytidine-mediated reductions in G9A histone methyltransferase and histone H3 K9 di-methylation levels are linked to tumor suppressor gene reactivation. Oncogene 2007;26:77–90.
26. Ushijima T, Watanabe N, Okochi E, Kaneda A, Sugimura T, Miyamoto K. Fidelity of the methylation pattern and its variation in the genome. Genome Res 2003;13:868–74.
27. Monte M, Simonatto M, Peche LY, et al. MAGE-A tumor antigens target p53 transactivation function through histone deacetylase recruitment and confer resistance to chemotherapeutic agents. Proc Natl Acad Sci U S A 2006;103:11160–5.
28. Naimi B, Latil A, Fournier G, Mangin P, Cussenot O, Berthon P. Down-regulation of (IIIb) and (IIIc) isoforms of fibroblast growth factor receptor 2 (FGFR2) is associated with malignant progression in human prostate. Prostate 2002;52:245–52.
29. Ricol D, Cappellen D, El Marjou A, et al. Tumour suppressive properties of fibroblast growth factor receptor 2-IIIb in human bladder cancer. Oncogene 1999;18:7234–43.
30. Bernard-Pierrot I, Ricol D, Cassidy A, et al. Inhibition of human bladder tumour cell growth by fibroblast growth factor receptor 2b is independent of its kinase activity. Involvement of the carboxy-terminal region of the receptor. Oncogene 2004;23:9201–11.
31. Kondo T, Zheng L, Liu W, Kurebayashi J, Asa SL, Ezzat S. Epigenetically controlled fibroblast growth factor receptor 2 signaling imposes on the RAS/BRAF/mitogen-activated protein kinase pathway to modulate thyroid cancer progression. Cancer Res 2007;67:5461–70.
32. Zhang Y, Wang H, Toratani S, et al. Growth inhibition by keratinocyte growth factor receptor of human salivary adenocarcinoma cells through induction of differentiation and apoptosis. Proc Natl Acad Sci U S A 2001;98:11336–40.
33. Xiao J, Chen HS. Biological functions of melanoma-associated antigens. World J Gastroenterol 2004;10:1849–53.
34. van der BP, Traversari C, Chomez P, et al. A gene encoding an antigen recognized by cytolytic T lymphocytes on a human melanoma. Science 1991;254:1643–7.
35. Weynants P, Lethe B, Brasseur F, Marchand M, Boon T. Expression of mage genes by non-small-cell lung carcinomas. Int J Cancer 1994;56:826–9.
36. Otte M, Zafrakas M, Riethdorf L, et al. MAGE-A gene expression pattern in primary breast cancer. Cancer Res 2001;61:6682–7.
37. Kim J, Reber HA, Hines OJ, et al. The clinical significance of MAGEA3 expression in pancreatic cancer. Int J Cancer 2006;118:2269–75.
38. Thapar K, Scheithauer BW, Kovacs K, Pernicone PJ, Laws ER, Jr. p53 expression in pituitary adenomas and carcinomas: correlation with invasiveness and tumor growth fractions. Neurosurgery 1996;38:765–71.
39. Sigalotti L, Fratta E, Coral S, et al. Intratumor heterogeneity of cancer/testis antigens expression in human cutaneous melanoma is methylation-regulated and functionally reverted by 5-aza-2′-deoxycytidine. Cancer Res 2004;64:9167–71.
40. Wischnewski F, Pantel K, Schwarzenbach H. Promoter demethylation and histone acetylation mediate gene expression of MAGE-A1, -A2, -A3, and -A12 in human cancer cells. Mol Cancer Res 2006;4:339–49.
41. Lloyd RV, Cano M, Landefeld TD. The effects of estrogens on tumor growth and on prolactin and growth hormone mRNA expression in rat pituitary tissues. Am J Pathol 1988;133:397–406.
42. Ezzat S, Asa SL. Mechanisms of disease: the pathogenesis of pituitary tumors. Nat Clin Pract Endocrinol Metab 2006;2:220–30.
43. Jacks T, Fazeli A, Schmitt EM, Bronson RT, Goodell MA, Weinberg RA. Effects of an Rb mutation in the mouse. Nature 1992;359:295–300.
44. Woloschak M, Yu A, Xiao J, Post KD. Abundance and state of phosphorylation of the retinoblastoma gene product in human pituitary tumors. Int J Cancer 1996;67:16–9.
45. Pei L, Melmed S, Scheithauer B, Kovacs K, Benedict WF, Prager D. Frequent loss of heterozygosity at the retinoblastoma susceptibility gene (RB) locus in aggressive pituitary tumors: evidence for a chromosome 13 tumor suppressor gene other than RB. Cancer Res 1995;55:1613–6.
46. Simpson DJ, Hibberts NA, McNicol AM, Clayton RN, Farrell WE. Loss of pRb expression in pituitary adenomas is associated with methylation of the RB1 CpG island. Cancer Res 2000;60:1211–6.
47. Bates AS, Farrell WE, Bicknell EJ, et al. Allelic deletion in pituitary adenomas reflects aggressive biological activity and has potential value as a prognostic marker. J Clin Endocrinol Metab 1997;82:818–24.
48. Nakayama K, Ishida N, Shirane M, et al. Mice

lacking p27Kip1 display increased body size, multiple organ hyperplasia, retinal dysplasia, and pituitary tumors. Cell 1996;85:707–20.

49. Bamberger CM, Fehn M, Bamberger AM, et al. Reduced expression levels of the cell-cycle inhibitor p27Kip1 in human pituitary adenomas. Eur J Endocrinol 1999;140:250–5.

50. Lidhar K, Korbonits M, Jordan S, et al. Low expression of the cell cycle inhibitor p27Kip1 in normal corticotroph cells, corticotroph tumors, and malignant pituitary tumors. J Clin Endocrinol Metab 1999;84:3823–30.

51. Zhang X, Sun H, Danila DC, et al. Loss of expression of GADD45 γ, a growth inhibitory gene, in human pituitary adenomas: implications for tumorigenesis. J Clin Endocrinol Metab 2002;87:1262–7.

52. Bahar A, Bicknell JE, Simpson DJ, Clayton RN, Farrell WE. Loss of expression of the growth inhibitory gene GADD45γ, in human pituitary adenomas, is associated with CpG island methylation. Oncogene 2004;23:936–44.

53. Qian ZR, Sano T, Yoshimoto K, et al. Inactivation of RASSF1A tumor suppressor gene by aberrant promoter hypermethylation in human pituitary adenomas. Lab Invest 2005;85:464–73.

54. Zhao J, Dahle D, Zhou Y, Zhang X, Klibanski A. Hypermethylation of the promoter region is associated with the loss of MEG3 gene expression in human pituitary tumors. J Clin Endocrinol Metab 2005;90:2179–86.

55. Yang B, O'Herrin S, Wu J, et al. Select cancer testes antigens of the MAGE-A, -B, and -C families are expressed in mast cell lines and promote cell viability *in vitro* and *in vivo*. J Invest Dermatol 2007;127:267–75.

Clinical Cancer Research

Fibroblast Growth Factor 2 and Estrogen Control the Balance of Histone 3 Modifications Targeting MAGE-A3 in Pituitary Neoplasia

Xuegong Zhu, Sylvia L. Asa and Shereen Ezzat

Clin Cancer Res 2008;14:1984-1996.